

Vacancy-Assisted Diffusion in Silicon: A Three-Temperature-Regime Model

Damien Caliste and Pascal Pochet*

Département de Recherche Fondamentale sur la Matière Condensée, SP2M/L_Sim, CEA/Grenoble, F-38054 Grenoble cedex 9, France
(Received 25 March 2005; revised manuscript received 19 December 2005; published 27 September 2006)

In this Letter we report kinetic lattice Monte Carlo simulations of vacancy-assisted diffusion in silicon. We show that the observed temperature dependence for vacancy migration energy is explained by the existence of three diffusion regimes for divacancies. This characteristic has been rationalized with an analytical model. In the intermediate temperature regime the divacancy dissociation plays a key role and an effective migration energy $E_v^m \sim 2$ eV is predicted, computed from either full *ab initio* values or mixed with experimental ones. The exact position of this temperature regime strongly depends on vacancy concentration. Previous contradictory experimental results are revisited using this viewpoint.

DOI: 10.1103/PhysRevLett.97.135901

PACS numbers: 66.30.Hs, 61.72.Ji, 61.72.Yx, 61.82.Fk

Quantitative understanding of intrinsic point defects in Si is a key feature in nanoelectronics. Although it has been studied for several decades [1], the activation energy of vacancy diffusion is still debated and strongly depends on the interstitial contribution used in the diffusion data analysis [2]. Besides, several studies give similar values for formation and migration energies (i.e., $E_f = 3.6$ eV [3] and $E_m = 0.45$ eV [4] but also reproduced by first principle calculations as shown in a recent review; see [5]). However, in a recent Letter, Bracht *et al.* [6] challenged both formation and migration energy values. Using radiation enhanced silicon self-diffusion experiments, they found $E_v^f = 2.1$ eV and $E_v^m = 1.8$ eV in the 1050–1150 K temperature range. They conclude that the temperature dependence of the thermodynamic properties of the vacancy is the consequence of a localized nature of the vacancy as proposed by Seeger and Chik [7]. This conclusion seems to be confirmed by Ranki and Saarinen [8] who estimated $E_v^f = 2.8$ eV and $E_v^m = 1.3$ eV from positron-annihilation measurements in a highly *P*-doped silicon in the 650–900 K temperature range. In this Letter we report the calculation of silicon diffusivity in the presence of divacancies. The contribution of divacancies to diffusion was already proposed by Van Vechten [9] to reanalyze the debated positron-annihilation measurements of Dannefaer *et al.* [3]. However, while Van Vechten proposed vacancy agglomeration into divacancy upon thermal annealing, we refer to the reverse phenomenon, i.e., divacancy dissociation. We found a temperature window where the effective migration energy for diffusion is ~ 2 eV. The exact temperature window position depends on vacancy steady-state concentration (resulting from, for instance, irradiation or doping [10]). Based on an analytical model of the former phenomenon, we propose that the discrepancies between various authors [4,6,8] should be assigned to different temperature ranges and steady-state vacancy concentrations in the experiments.

We performed kinetic lattice Monte Carlo (KLMC) calculations to simulate atomic scale diffusion in silicon. All simulation boxes contain 2 vacancies. The largest box

counts up to 18×10^6 Si atoms, which corresponds to a vacancy concentration $C_v = 10^{-7}$ at⁻¹ that is in the range of the lowest vacancy concentration measurable by positron annihilation [8]. We checked that our results are independent from starting configurations (separated or assembled vacancies). The vacancy diffusivity $D_v(T)$ is obtained using the Einstein formula and averaging among 20 trajectories. The underlying energetic model is mainly supported by an *ab initio* database. It is built from density functional theory within local density approximation calculations done with the plane-wave code CPMD v3.8 [11] and the Hartwigsen-Goedecker-Hutter pseudopotentials [12]. The *ab initio* supercell consists of 216 Si sites with a Si-Si bond distance of 2.35 Å. Calculations were done at the Γ point with 340 eV of cutoff, and atomic positions are relaxed. These parameters have proved to give good convergence for the system of vacancies in silicon [13]. The barriers are computed using the nudged elastic band (NEB) [14,15] method coupled with direct inversion in the iterative subspace [16] relaxation.

The energetic model underlying the KLMC calculations is built to take into account the interactions between 2 vacancies, up to the third nearest-neighbor (NN) position (see Fig. 1). It implies three possible energy levels for two vacancies in silicon: a divacancy (where the two vacancies are 1NN), two vacancies positioned as 2NN, and two isolated vacancies (which means that n NN positions with $n > 2$ are energetically equivalent in our model). The associated *ab initio* formation energies are the following ones: $E(1\text{NN}) = E_{2v}^f = 5.26$ eV, $E(2\text{NN}) = 6.45$ eV, and $E(3\text{NN}) = 2E_{1v}^f = 7.12$ eV. These values are in good

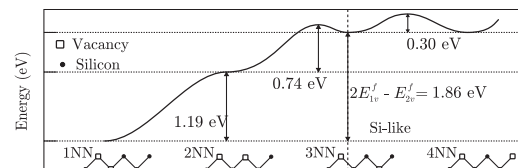


FIG. 1. Energies for states and barriers as used in the KLMC calculations. The represented path is a divacancy dissociation.

agreement with the experimental ones [3,17]. To express the kinetic, three movements are also required: the first is the monovacancy hopping, featuring $E_{1v}^m = 0.30$ eV. We assume that it occurs as soon as vacancies are 3NN from each other (the difference with *ab initio* is less than 0.15 eV [18]). The second is the dissociation as shown in Fig. 1 and is modeled by two steps, going from 1NN to 3NN with two consecutive jumps with energies of 1.19 and 0.74 eV, respectively. The last is a divacancy motion going from 1NN to another shifted 1NN position. In the KLMC, the 2NN position is used as an intermediate transition. It corresponds to an *ab initio* direct divacancy migration barrier of $E_{2v}^m = 1.19$ eV close to the 1.35 eV found by Hwang and Goddard III [18].

Since vacancy migration is the key parameter of this study, the value of 0.45 eV experimentally obtained by Watkins *et al.* [4] will be used for most calculations, instead of the *ab initio* value of 0.30 eV. The precise influence of this parameter has been checked, and the *ab initio* value has also been used in selected cases [see Fig. 3(b)].

The diffusivity as a function of temperature and at various vacancy concentrations is reported in Fig. 2. The results are normalized with the vacancy concentration in the simulation box $C_v^* (= \frac{2}{N})$. Three temperature regions can be defined. At low temperatures (labeled region III), the divacancy is stable and dominates the diffusion with an activation energy of 1.25 eV. At high temperatures (labeled region I), monovacancies control the diffusion, $\tilde{E}^m = 0.46$ eV. An intermediate temperature range (labeled

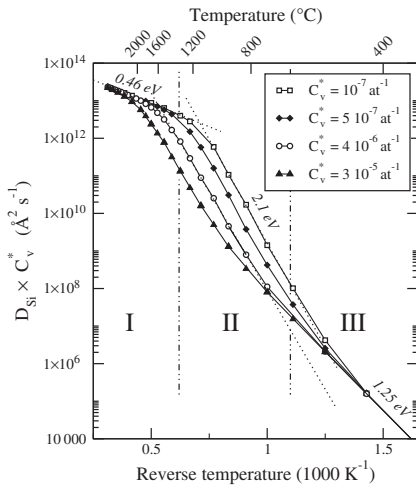


FIG. 2. Silicon diffusivity D_{Si} versus reverse temperature for various vacancy concentrations as measured from KLMC simulations with $E_{1v}^m = 0.45$ eV. Three temperature regions are evidenced and different states are activated: monovacancy in region I (high temperature), divacancy in region III (low temperature), and both in region II (intermediate temperature). The resulting effective migration energy in this region is connected to divacancy dissociation that rules the fraction of time between mono- and divacancy diffusion (see text).

region II) is revealed between the two previous regions. In this range both mono- and divacancies are present, but monovacancies are the principal responsible for Si diffusion. An effective activation energy of ~ 2.1 eV is measured for all KLMC simulations whatever the concentration value. The exact position of region II depends on the vacancy concentration. For steady-state vacancy concentration in the experimental range ($\sim 1 \times 10^{-7}$ at $^{-1}$ [8]), region II is between 900 and 1300 K, while for higher vacancy concentrations, the high temperature boundary $T_{\text{I-II}}$ is shifted toward higher temperatures.

This *three-temperature-regime* behavior is rationalized using an analytical model accounting for that mixed diffusion regime. The effective diffusivity \tilde{D} can be formulated as

$$\tilde{D}(T, C_v^*) = f_\tau(T, C_v^*) \times D_{1v}(T) + [1 - f_\tau(T, C_v^*)]D_{2v}(T), \quad (1)$$

where f_τ is the time fraction of separate vacancy diffusion at D_{1v} ($1 - f_\tau$ for divacancy at D_{2v}).

In a Boltzmann repartition model, f_τ is given by the ratio of the monovacancy concentration divided by the sum of both monovacancy and divacancy concentrations. Configurational entropies [$k_b \ln(\tilde{C})$] can be simply estimated by counting the number of possibilities to arrange two vacancies in a box of N sites featuring the diamond lattice, which leads to $\tilde{C} = \frac{N(N-5)}{2}$ for the two monovacancies and $\tilde{C} = \frac{4N}{2}$ for the divacancy. We get after simplifications (assuming $C_v^* = \frac{2}{N}$)

$$f_\tau(T, C_v^*) = \frac{1}{1 + 2C_v^* e^{\beta(2E_{1v}^f - E_{2v}^f)}}. \quad (2)$$

The effective migration energy is obtained from the $\beta (= \frac{1}{k_b T})$ derivative of $\ln(\tilde{D})$:

$$\tilde{E}^m(T, C_v^*) = f_a E_{1v}^m + f_b (2E_{1v}^f - E_{2v}^f) + (1 - f_a) E_{2v}^m, \quad (3)$$

$$\text{with } f_a(T, C_v^*) = \frac{D_{1v} f_\tau}{D_{1v} f_\tau + D_{2v} (1 - f_\tau)}$$

$$\text{and } f_b(T, C_v^*) = f_a - f_\tau.$$

The three functions f_a , f_b , and f_τ are $[0, 1]$ bounded. f_a and f_τ are monotonous functions, while f_b is a Gaussian-like function. At high temperature $f_\tau \approx f_a \approx 1$ and $f_b \approx 0$, so the right-hand side (r.h.s.) of Eq. (3) reduces to its first term E_{1v}^m : divacancies are dissociated and the atomic diffusion is assisted only by monovacancies. At low temperature $f_a \approx f_b \approx f_\tau \approx 0$, so the r.h.s. of Eq. (3) reduces to its last term E_{2v}^m : divacancies are strongly associated and the diffusion is assisted only by divacancies. There is an intermediate temperature range where $D_{2v} \ll D_{1v} f_\tau$. In this region f_a is then shifted to lower temperature with respect to f_τ , and thus we get $f_\tau \approx 0$ and $f_b \approx f_a \approx 1$;

Eq. (3) is then approached by

$$\tilde{E}^m \simeq 2E_{1v}^f - E_{2v}^f + E_{1v}^m. \quad (5)$$

This depicts the fact that even with the existence of divacancies, the Si diffusion is mostly driven by monovacancy migration and the cost of repeated dissociations also has to be taken into account.

The effective migration for silicon as a function of the temperature is reported in Fig. 3(a) for two selected vacancy concentrations. The agreement with the effective migration computed from Eq. (3) is very good for both reported vacancy concentrations. Additional KLMC simulations performed using $E_{1v}^m = 0.3$ eV (i.e., the *ab initio* value) are depicted in Fig. 3(b) for $C_v^* = 5 \times 10^{-7}$ at⁻¹. In regions II and I, effective diffusion energy depends on E_{1v}^m and is indeed shifted (respectively, from 2.1 to 2.0 eV and from 0.46 to 0.32 eV), but the localizations of the three regions are not significantly altered. In both graphs, the effective diffusion energy plotted from the KLMC calculations is noisy as being the derivative value of curves plotted on Fig. 2. According to Eq. (5) one would expect in region II an effective migration energy of 2.3 eV (when $E_{1v}^m = 0.45$ eV) featuring a kind of plateau but instead 2.1 eV is measured as reported with the dotted line in Fig. 2. This small difference between the KLMC calculation and the theoretical value should be assigned to the improper migration saddle point for divacancy migration introduced in the KLMC model.

However, the main feature of our KLMC simulations (giving a high value for $\tilde{E}^m \sim 2$ eV in region II) fits well with our analytical model, either with complete *ab initio* parameters or using the experimental value for E_{1v}^m . Moreover, in a recent molecular dynamics study [19], the increase of the effective migration energy from 1.3 eV at

low temperature to a value ~ 2 eV at higher temperature has been already observed for divacancies and can be understood with our three-temperature-regime model [Eq. (5) gives 1.9 eV for the parameters they used [19]]. The third region has not been investigated in these simulations since the vacancy concentration was too high and region I would have been above the melting temperature (1683 K).

Up to now we have obtained a very good description of our KLMC simulations using our three-temperature-regime model. However, in both KLMC simulations and the model, the total vacancy concentration C_v^* is temperature independent, unlike in experiments. The model thus needs to be extended to allow comparisons with experiments. This is achieved when considering a grand canonical ensemble with two reservoirs, one for vacancies and another one for divacancies. Since divacancies are mostly formed at equilibrium by monovacancy association, we consider a chemical potential for divacancy formation equal to twice the value of the chemical potential for monovacancy formation. The fraction for separate vacancy diffusion f_τ exactly writes as in Eq. (2) with C_v now being temperature dependent.

The β derivative of $\ln\{\tilde{D}[T, C_v(T)]\}$ leads to a modified equation for the effective migration energy:

$$\tilde{E}_{\text{th}}^m[T, C_v(T)] = \tilde{E}^m[T, C_v(T)] + f_b \frac{\partial \ln C_v(T)}{\partial \beta}. \quad (6)$$

\tilde{E}^m has the same formulation as in Eq. (3) with f_a, f_b , and f_τ being now temperature dependent through $C_v(T)$. This dependency adds an extra contribution to \tilde{E}_{th}^m : $\hat{E}^m = f_b \frac{\partial \ln C_v(T)}{\partial \beta}$. A model for the total vacancy concentration is then needed to go beyond Eq. (6). The total vacancy concentration can be written as the sum of the steady-state excess vacancy (e.g., due to irradiation) C_v^{forcing} and the thermal vacancy concentration $C_v^{\text{th}}(T)$. The extra contribution \hat{E}^m to the effective migration energy is then equal to

$$\hat{E}^m = \frac{-E_{1v}^f f_b}{1 + \gamma}, \quad \text{with} \quad \gamma = \frac{C_v^{\text{forcing}}}{C_v^{\text{th}}(T)}. \quad (7)$$

Under high forcing ($\gamma \gg 1$) and for all temperatures, $\hat{E}^m \simeq 0$, so we find again the first simple model underlying Eq. (3). Under very low forcing, the ratio, $\gamma \ll 1$, so $\hat{E}^m \simeq -E_{1v}^f f_b$. In the latter condition, using for $C_v^{\text{th}}(T)$ the vacancy formation energy and entropy as proposed by Bracht *et al.* [20], regions III and II are pushed back to low temperatures. Consequently, a monovacancy diffusion with a migration energy of E_{1v}^m is found over all the temperature ranges. This is consistent with the experimental observations at equilibrium or at low forcing like in the pioneer work of Watkins *et al.* [4].

The next step is to check the ability of this model to reproduce previous experimental results [6,8] where

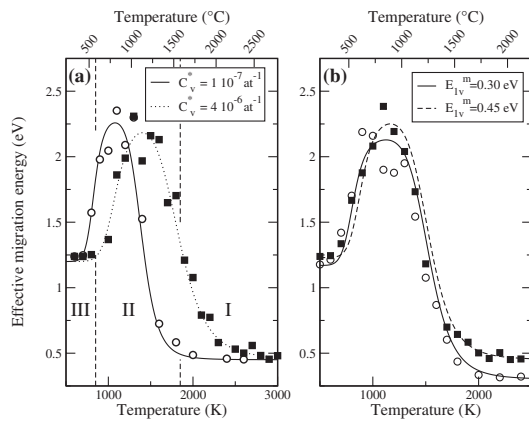


FIG. 3. Effective migration energies for silicon diffusion evaluated from the KLMC simulations as a function of temperature (a) at $C_v^* = 1 \times 10^{-7}$ at⁻¹ (squares) and 4×10^{-6} at⁻¹ (circles) with $E_{1v}^m = 0.45$ eV; (b) at $C_v^* = 5 \times 10^{-7}$ at⁻¹ with $E_{1v}^m = 0.30$ eV (circles) and $E_{1v}^m = 0.45$ eV (squares). The lines are computed from Eq. (3) using corresponding values.

C_v^{forcing} is significant. For this purpose we use the model, keeping all parameters equal to the main values used in the KLMC simulations, the only parameter to be fitted (or extracted for the experimental setup) being the steady-state vacancy concentration C_v^{forcing} . This stands for the residual vacancies at steady state induced by irradiation after recombination with interstitials or microstructure.

In their Letter Ranki and Saarinen [8] claimed that the minimum vacancy concentration C_v they could detect with positron annihilation is higher than 2×10^{-7} at $^{-1}$. In this experiment, the vacancy supersaturation is induced by the high dopant concentration [10]. The effective migration energy is measured in the range 650–900 K corresponding to region III for this vacancy concentration [Eq. (6) gives, for $C_v^{\text{forcing}} \geq 2 \times 10^{-7}$ at $^{-1}$, $T_{\text{III-II}} \geq 850$ K]. They found 1.2 eV for the highly doped silicon and estimated [8] a value of 1.3 eV in an intrinsic silicon. The latter value perfectly fit to the divacancy migration as predicted by our model in this temperature range.

In the Letter of Bracht *et al.* [6], the vacancy concentration is increased by means of 2 MeV proton irradiation. From a careful analysis of the irradiation conditions and assuming a quite reasonable capture radius for mutual vacancy-interstitial recombination, Bracht *et al.* [6] estimate the net production rate for vacancies to be between 2.6×10^{-7} and 6.4×10^{-8} s $^{-1}$. The steady-state vacancy concentration C_v^{forcing} during their experiment should be in the same range for which Eq. (6) gives $T_{\text{III-II}}$ between 800 and 850 K and $T_{\text{II-I}}$ between 1350 and 1450 K. Thus their experimental temperature range 1050–1150 K is clearly in region II. So their 1.8 eV \pm 0.5 eV measurement would correspond the divacancy dissociation regime as predicted by our model.

Although in experiments vacancy diffusion is sensitive to many aspects (interstitial or impurity interaction) that are not considered in our three-temperature-regime model for divacancy diffusion, it gives a consistent view of these three apparently scattered experimental results [4,6,8] as far as extracted vacancy diffusion data are concerned. In addition, such a three-temperature-regime behavior has been observed by David *et al.* [21] in silicon under He implantation. In these experiments, divacancies are known to contribute to He clustering. The observed mean radius evolution of cavity as a function of implantation temperature is analyzed with divacancy and monovacancy diffusion for stages III and I, respectively, while stage II is not well understood. Our three-temperature-regime model gives then a coherent diffusion framework for the three observed stages.

In conclusion, our investigation of vacancy-assisted self-diffusion in silicon gives a simple but strong explanation to the observed [6,7,20] temperature variations of vacancy migration energy. Our KLMC simulations reveal an intermediate diffusion regime where divacancy dissociation is

involved. The high effective migration within this regime is a function of migration and formation energies of mono- and divacancies [Eq. (5)]. The exact temperature range of this regime depends strongly on steady-state vacancy concentration. The latter correlation explains the discrepancies between several measurements for which various radiation conditions (or dopant concentration) involving different vacancy concentrations were used.

Useful discussions with Dr. T. Deutsch and Dr. F. Lançon are gratefully acknowledged. We would also like to thank C. Sbraccia for his scripts that implement the NEB method.

*Corresponding author.

Electronic address: pascal.pochet@cea.fr

- [1] G.D. Watkins and J.W. Corbett, Phys. Rev. **134**, A1359 (1964).
- [2] H. Bracht, Physica (Amsterdam) **376B–377B**, 11 (2006).
- [3] S. Dannefaer, P. Mascher, and D. Kerr, Phys. Rev. Lett. **56**, 2195 (1986).
- [4] G.D. Watkins, J.R. Troxell, and A.P. Chatterjee, in *Defects and Radiation Effects in Semiconductors, 1978*, edited by J.H. Albany (Institute of Physics, London, 1979), Chap. 1, pp. 16–30.
- [5] F. El-Mellouhi, N. Mousseau, and P. Ordejon, Phys. Rev. B **70**, 205202 (2004), and references therein.
- [6] H. Bracht, J.F. Pedersen, N. Zangenberg, A.N. Larsen, E.E. Haller, G. Lulli, and M. Posselt, Phys. Rev. Lett. **91**, 245502 (2003).
- [7] A. Seeger and K.P. Chik, Phys. Status Solidi **29**, 455 (1968).
- [8] V. Ranki and K. Saarinen, Phys. Rev. Lett. **93**, 255502 (2004).
- [9] J.A. Van Vechten, Phys. Rev. B **33**, 2674 (1986).
- [10] P.M. Fahey, P.B. Griffin, and J.D. Plummer, Rev. Mod. Phys. **61**, 289 (1989).
- [11] CPMD, Copyright IBM Corp. (1990–2001); Copyright MPI für Festkörperforschung Stuttgart (1997–2001).
- [12] C. Hartwigsen, S. Goedecker, and J. Hutter, Phys. Rev. B **58**, 3641 (1998).
- [13] M.I.J. Probert and M.C. Payne, Phys. Rev. B **67**, 075204 (2003).
- [14] G. Henkelman, B.P. Uberuaga, and H. Jónsson, J. Chem. Phys. **113**, 9901 (2000).
- [15] G. Henkelman and H. Jónsson, J. Chem. Phys. **113**, 9978 (2000).
- [16] P. Pulay, Chem. Phys. Lett. **73**, 393 (1980).
- [17] G.D. Watkins and J.W. Corbett, Phys. Rev. **138**, A543 (1965).
- [18] G.S. Hwang and W.A. Goddard III, Phys. Rev. B **65**, 233205 (2002).
- [19] M. Prasad and T. Sinno, Phys. Rev. B **68**, 045206 (2003).
- [20] H. Bracht, N. Stolwijk, and H. Mehrer, Phys. Rev. B **52**, 16 542 (1995).
- [21] M.L. David, M.F. Beaufort, and J.F. Barbot, J. Appl. Phys. **93**, 1438 (2003).